Molecular and Cellular Endocrinology 607 (2025) 112602

Contents lists available at ScienceDirect

Molecular and Cellular Endocrinology

journal homepage: www.elsevier.com/locate/mce

Sarcospan, a candidate gene of fat distribution, may affect lipid storage in adipocytes

Katharina Anastasia Dinter [a], Samantha Aurich [a,b], Luise Müller [a], Adhideb Ghosh [c], Falko Noé [c], Christian Wolfrum [c], Matthias Blüher [a,d], Anne Hoffmann [d], Peter Kovacs [a,e], Maria Keller [a,d,*]

[a] *Medical Department III – Endocrinology, Nephrology, Rheumatology, University of Leipzig Medical Center, Leipzig, 04103, Germany*
[b] *Department of Animal Physiology, Faculty of Life Sciences, University of Leipzig, Leipzig, 04103, Germany*
[c] *Institute of Food, Nutrition and Health, ETH Zürich, Schwerzenbach, 8092, Switzerland*
[d] *Helmholtz Institute for Metabolic, Obesity and Vascular Research (HI-MAG) of the Helmholtz Center Munich at the University of Leipzig and University Hospital Leipzig, Leipzig, 04103, Germany*
[e] *Deutsches Zentrum für Diabetesforschung e.V., Neuherberg, 85764, Germany*

ARTICLE INFO

Keywords:
Obesity
Adipocytes
Adipose tissue
Adipogenesis
Small interfering RNA
CRISPR
DNA methylation

ABSTRACT

Background and aims: Genetic and epigenetic variations in the *Sarcospan* (*SSPN*) gene are associated with parameters of fat distribution (body mass index, waist-to-hip ratio), glucose homeostasis and adipocyte size in human potentially by affecting adipogenesis. This study aims at clarifying the impact of *SSPN* on adipogenesis, particularly focusing on its promoter methylation.
Materials and methods: Immortalized murine epididymal preadipocytes were transfected with fluorescence-marked plasmids coding for DNMT3a, CRISPR/dCas9-Suntag and vectors carrying guide RNAs complementary to the transcription start site region and differentiated to mature adipocytes. We performed siRNA-mediated *Sspn* knockdown in epididymal preadipocytes, measured target DNA methylation using pyrosequencing and quantified transcriptional changes of *Sspn* and adipogenic genes by qPCR. Additionally, we correlated *SSPN* mRNA values and clinical characteristics from a large human adipose tissue biobank (Leipzig Obesity Biobank).
Results: Epigenetic editing of the *Sspn* regulatory region in preadipocytes resulted in a significant increase (up to 35 %) in DNA promoter methylation throughout adipocyte differentiation but showed only minor effects on *Sspn* expression and fat storage. Though siRNA knockdown could also not contribute to understand the role of *Sspn* in a 2D adipogenesis model, large-scale correlation analyses still indicate the gene to be a key player in fat distribution and glucose homeostasis.
Conclusions: Although the epigenetic downregulation of *Sspn* showed only marginal effects on adipogenesis, associations of *SSPN* expression in human adipose tissue with parameters of fat distribution and glucose homeostasis make it a promising candidate for further studies addressing metabolic processes in adipose tissue.

1. Introduction

As obesity and its comorbidities represent one of the major health burdens in our current society, understanding why some individuals seem to have a higher risk to be affected by metabolic disruptions than others is a significant goal. Increased energy uptake based on high caloric meals and reduced energy consumption due to an inactive lifestyle together led to an energy imbalance which represents the main driver of a massive adipose tissue expansion. Fat will either be stored subcutaneously or in abdominal visceral regions, with the latter going hand in hand with an increased risk for cardiometabolic and cardiovascular diseases (Hiuge-Shimizu et al., 2012; Neeland et al., 2012, 2013, 2015). Visceral obesity goes in line with an ectopic fat accumulation nearby major organs such as the liver or pancreas, further triggering dysregulated adipokine secretion, enhanced fatty acid release and low-grade inflammation (Wajchenberg, 2000; Tchernof and Després, 2013), which finally results in an increased risk to develop type 2 diabetes (Stefan, 2020). Besides a sedentary lifestyle, adipose tissue distribution might to some extent be regulated by genetic predispositions and epigenetic mechanisms (Rohde et al., 2019). Among

* Corresponding author. Helmholtz Institute for Metabolic, Obesity and Vascular Research (HI-MAG) of the Helmholtz Center Munich at the University of Leipzig and University Hospital Leipzig, Philipp-Rosenthal Str. 27, D-04103 Leipzig, Germany.
E-mail address: maria.keller@helmholtz-munich.de (M. Keller).

https://doi.org/10.1016/j.mce.2025.112602
Received 27 February 2025; Received in revised form 2 May 2025; Accepted 7 June 2025
Available online 7 June 2025

others, genome-wide association studies described a single nucleotide polymorphism (SNP; rs718314) in an intergenic region between the *Sarcospan* (*SSPN*) locus and the *Inositol 1,4,5-Trisphosphate Receptor Type 2* (*ITPR2*) locus to be significantly associated with waist-to-hip ratio (WHR) (Heid et al., 2010; Liu et al., 2013; Shungin et al., 2015).

SSPN was discovered particularly late (Crosbie et al., 1997) as a member of the dystrophin glycoprotein complex (DGC), which performs important functions in anchoring the extracellular matrix to the cytoskeleton (Marshall et al., 2012a). The transmembrane protein as small as 25 kDa is expressed ubiquitously, for instance in subcutaneous adipose tissue (SAT), omental visceral adipose tissue (OVAT), aorta or nerve (The Genotype, 2013), but is especially known for its effects in skeletal muscle. Through a complex interplay with the other components of the DGC at the cell membrane, *SSPN* contributes to normal muscle function (Marshall et al., 2012b). Under conditions of muscular dystrophy, *SSPN* overexpression is to a certain extent capable to "rescue" muscle function by favorably influencing several pathways (Marshall et al., 2012a; Peter et al., 2008; Marshall and Crosbie-Watson, 2013). The observation that in human muscular dystrophy, muscle cells are partially replaced by fibroblasts and adipocytes (Ceco and McNally, 2013) and its association with WHR imply that *SSPN* might play a role in adipogenesis.

Voisin et al. revealed an association of the G allele at rs718314 with *SSPN* promoter methylation at the CpG site cg02058108 (Voisin et al., 2015), suggesting an underlying epigenetic regulation mechanism. This was further supported by an epigenome-wide association analysis for promoter methylation in adipose tissue, which showed *SSPN* to be the candidate most significantly correlated with body mass index (BMI) in SAT (Keller et al., 2017). Furthermore, *SSPN* promoter methylation displayed significant negative relationships with parameters of fat distribution and glucose homeostasis such as waist circumference, WHR, fasting plasma insulin (FPI) and HbA1c in SAT and free fatty acids in OVAT (Keller et al., 2017). *SSPN* promoter methylation also differs between obese and non-obese individuals in OVAT (Keller et al., 2017), correlates negatively with mRNA expression and is associated with the maximum adipocyte size in SAT (Keller et al., 2018). Accordingly, Groh et al. showed that white adipose tissue from mice, which lacked both the DGC member β-sarcoglycan and Sspn display microscopic features of lipodystrophy (Groh et al., 2009).

Collectively, these findings raise the question of whether hypermethylation of the *SSPN* DNA promoter at previously identified target sites may suppress its mRNA expression, thereby impacting adipogenesis and fat storage. To explore this hypothesis, we examined the association between *SSPN* mRNA expression in adipose tissue and various metabolic traits. Additionally, we employed an *in vitro* epigenetic editing approach using a CRISPR/dCas9 system in murine epididymal preadipocytes to directly assess the functional consequences on adipocyte differentiation.

1.1. Study design and methods

The detailed study design is depicted in Fig. 1. Briefly, immortalized murine preadipocytes underwent sequence-specific hypermethylation at the *SSPN* promoter using an established CRISPR/dCas9 system (Pflueger et al., 2018) including transfection followed by FACS sorting with a triple positive (GFP, mCherry and BFP) fluorescence strategy. Triple positive living cells were then expanded and differentiated into mature adipocytes to investigate the functional effects on adipocyte differentiation and fat storage.

1.1.1. Cell culture and maintenance

Immortalized epididymal murine preadipocytes, obtained by collagenase digestion of white adipose tissue with subsequent incubation with a retroviral vector encoding the SV40T antigen and kindly provided by Prof. Klein and Dr. Perwitz from Lübeck (Kovsan et al., 2009), at passage 11 to 15 were cultured in Dulbecco's Modified Eagle Medium (DMEM, high glucose, high pyruvate, Gibco/Thermofisher Scientific; Waltham, Massachusetts, USA) with 10 % Fetal Bovine Serum (FBS, Gibco/Thermofisher Scientific) and 1 % Penicillin/Streptomycin (Gibco/Thermofisher Scientific) and kept at 37 °C and 5 % CO2.

1.1.2. Plasmid selection and preparation

Two previously described CpG regions in the human *SSPN* promoter (Keller et al., 2018) were chosen and aligned to the mouse genome using the UCSC epigenome browser BLAT tool (genome.ucsc.edu) (Kuhn et al., 2013). Since the promoter has a slightly different structure in mouse (Fig. 1A), one of these regions is hypermethylated (mean methylation at 99.34 %) in epididymal adipocytes and therefore presumably upstream the promoter region. Thus, we chose the region in close proximity to the transcription start site (chr6: 145934023–145934099) and designed two guide RNAs (gRNAs) complementary to the target DNA region using the CRISPOR Tool (http://crispor.tefor.net) (Concordet and Haeussler, 2018) based on the calculated specificity-, efficiency- and out-of-frame score, avoiding low score values and thereby potential off-target effects in the mouse genome (see Fig. 1 and Supplemental Table 1).

Plasmids were chosen according to Pflueger et al. (2018) following the dCas9-SunTag-DNMT3A protocol. This includes one plasmid containing a single chain variable fragment antibody GCN4 fused to DNA

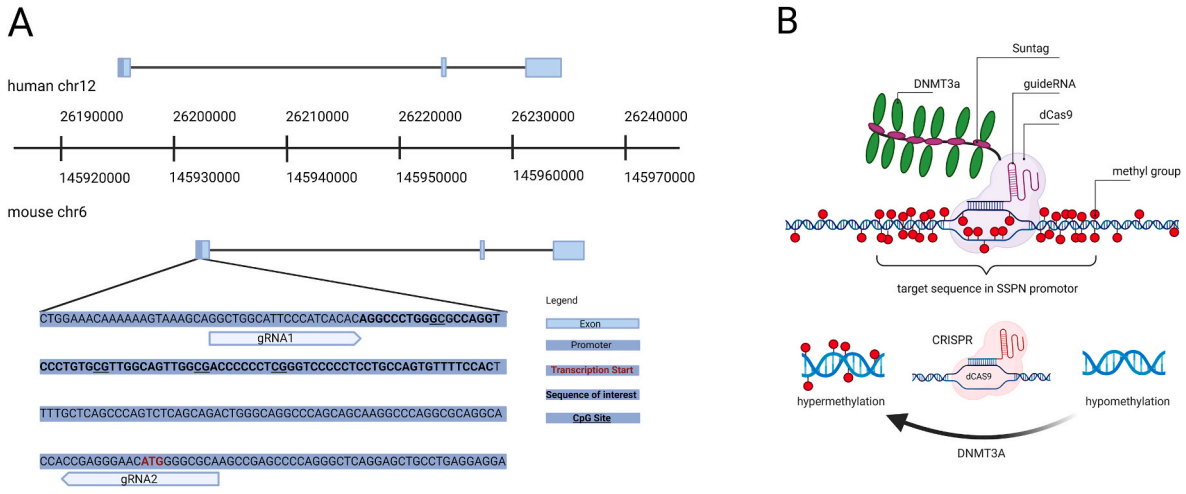

Fig. 1. Graphical representation of the methods used. A) Position of the target region within the *Sspn* promoter and binding sites of the two guide RNAs. B) Schematic display of the structure of the CRISPR/dCas9-DNMT3a construct for hypermethylation of the target sequence. Images were created using Biorender.com with the inclusion of information from the UCSC genome browser (genome.ucsc.edu, accessed on June 8, 2023).

methyltransferase 3a (DNMT3A-pEF1a-NLS-scFvGCN4-DNMT3a, GFP-labeled), one plasmid coding for the dCas9-SunTag-construct (pGK-dCas9-Suntag, BFP-labeled) and one plasmid containing an empty gRNA scaffold driven by a U6 promoter (pEF1a-mCherry-EMPTY-gRNA). All plasmids were gifts from the Ryan Lister lab (Pflueger et al., 2018) and purchased via Addgene (Watertown, Massachusetts, USA). A schematic depiction of the function of the individual elements encoded by the plasmids used can be seen in Fig. 1B. In short, the gRNAs lead the construct consisting of dCas9 and a chain of multiple DNMT3a methylation enzymes to the target sequence, the binding of which induces hypermethylation of the region.

The pEF1a-mCherry-EMPTY-gRNA plasmid was used as a negative control (without gRNA) and as a gRNA-delivering plasmid. To obtain pEF1a-mCherry-gRNA plasmids, single stranded gRNA oligonucleotides were amplified to double stranded guide-oligos using Q5 High-Fidelity DNA Polymerase (New England Biolabs; Ipswich, Massachusetts, USA), cloned into the EMPTY-gRNA plasmid using the Gibson Assembly Cloning kit (New England Biolabs) after linearization by Afl II (New England Biolabs) restriction digestion.

1.1.3. Cell transfection

One million cells were transfected with 2.5 µg of each pEF1a-mCherry-gRNA plasmid, 5 µg of pEF1a-NLS-scFvGCN4-DNMT3a and 5 µg of pGK-dCas9-Suntag-BFP using the NeonTM electroporation system (Invitrogen/Thermofisher Scientific; Waltham, Massachusetts, USA) at 1300 V for 20 ms two times (*Sspn* gRNAs). For the Plasmid Control, cells were transfected equally, but the pEF1a-mCherry-gRNA plasmid was substituted by 5 µg of pEF1a-mCherry-EMPTY-gRNA. We further included an impulse control (Imp), where the same number of cells was electroporated without addition of any plasmids as well as an untreated control (UT) without electroporation.

24 h post transfection, *Sspn* gRNAs and Plasmid Control cells were FACS sorted for triple positive cells containing mCherry, BFP and GFP fluorescence signals, while Imp cells were FACS sorted for viable cells only and UT cells were not sorted. Subsequently, they were cultured in standard medium supplemented with 1 % Penicillin/Streptomycin (Gibco/Thermofisher Scientific) for another one to four days to gain enough cell material for differentiation.

1.1.4. Adipocyte differentiation

After FACS sorting, cells were seeded into either 12-well or 6-well plates and cultured until confluence. Afterwards, cells were differentiated as follows: 24 h after cells reached 100 % confluence (day zero), all cells were placed in induction medium containing DMEM with 10 % FBS supplemented with 20 nM insulin (Roche; Basel, Switzerland), 1 nM triiodothyronine (T3, Sigma Aldrich/Merck; Taufkirchen, Germany), 2 µM/ml dexamethasone (Sigma Aldrich/Merck), 0,125 mM indomethacin (Sigma Aldrich/Merck) and 500 µM 3-Isobutyl-1-methylxanthine (IBMX, Sigma Aldrich/Merck). On day two, medium was changed to differentiation medium containing DMEM with 10 % FBS, 20 nM insulin and 500 µM T3. On day four, cells went back on a standard medium (DMEM with 10 % FBS) without other additives. Similarly, the experiments were also carried out in inguinal preadipocytes (see Supplements). Preadipocyte transfections and differentiations were replicated three times.

1.2. DNA and RNA isolation

DNA was extracted on days zero, four and eight using the DNeasy Blood & Tissue Kit (Qiagen; Venlo, Netherlands) following the manufacturer's instructions. DNA concentrations were measured with the NanoDrop 2000 spectral photometer (Thermofisher Scientific). RNA was isolated simultaneously using the RNeasy Mini Kit (Qiagen) according to the manufacturer's guidelines and including a DNAse (Qiagen) digestion and quantified with the NanoDrop 2000 spectral photometer.

1.3. DNA methylation analysis

First, DNA samples were bisulfite converted using the EpiTect Fast DNA Bisulfite Kit (Qiagen). Subsequent PCR was performed in duplicates with self-designed primers flanking the sequence of interest (Supplemental Table 1) for each sample, including non-template controls. PCR products were controlled regarding purity and integrity using agarose gel electrophoresis.

Finally, DNA methylation was quantified with the PyroMark Q24 pyrosequencing system including the PyroMark Gold Q24 Reagents (Qiagen). Results were analyzed with the corresponding PyroMark Q24 software and methylation values of medium to poor quality were excluded, leaving only measurements of high quality in the analysis.

1.4. mRNA expression analysis

For mRNA quantification 500 ng of each RNA sample were converted into cDNA using the SuperScript III Reverse Transcription Kit (Invitrogen) according to the manufacturer's instructions. Additionally, RNAse H (Invitrogen) was added to the reactions to eliminate remaining mRNA while cDNA is synthesized. Next, quantitative real time PCR (qPCR) was performed with the QuantStudio 6 system (Thermofisher Scientific) using the GoTaq Probe qPCR Master Mix (Promega) containing the ROX dye as well as probes for *Sspn* (Mm00447794_m1), *CCAAT/enhancer-binding protein beta (Cebpb;* Mm00843434_s1), *Adiponectin (Adipoq*; Mm00456425_m1), *Peroxisome proliferator-activated receptor gamma (Pparg*; Mm01184322_s1) as well as *Glyceraldehyde-3-phosphate (Gapdh*; Mm99999915_g1) and *Ribosomal protein lateral stalk subunit P0 (Rplp0;* Mm00725448_s1) (Thermofisher Scientific). Measurements were performed in triplicates and non-template controls as well as non-enzyme controls obtained from the reverse transcription were carried along to exclude contaminations. Efficiencies were determined by use of a standard curve and an efficiency-based formula (Pfaffl, 2001) was used to calculate an mRNA expression ratio relative to *Rplp0* as the reference gene in duplicates per plate and gene.

1.5. Fluorescence spectroscopy and fluorescence microscopy

To evaluate adipogenesis progression based on epigenetic modifications in the *Sspn* promoter, cells were seeded into 96-well plates for each treatment and cell line, differentiated as described, and stained on days zero, four, and eight with AdipoRed Assay reagent (Lonza; Basel, Switzerland) to quantify lipid content and Hoechst 33342 (Thermofisher Scientific) to mark nuclear structures with fluorescence signals normalized to cell number using a Spark Multimode Microplate Reader (Tecan Group; Männedorf, Switzerland; AdipoRed: excitation 485 nm, emission 535 nm; Hoechst 33342: excitation 361 nm, emission 486 nm).

In addition, cells for fluorescence microscopy were cultured on 12-well plates and stained in the same way as for spectroscopy. Images of the so treated cells were taken using the Carl Zeiss Axio Observer (Zeiss; Oberkochen, Germany) to illustrate the proportion of nuclei and increasing lipid content. Images of the cells were also repeatedly taken under the brightfield microscope (Carl Zeiss Axio Vert.A1; Zeiss).

1.6. siRNA-induced Sspn knockdown

Epididymal cells were seeded onto 12-well plates 24 h prior to siRNA delivery using serum-reduced medium (DMEM with 2 % FBS), as siRNA uptake can be inhibited by bovine serum albumin.

For transfection, a 100 µM Accell™ siRNA (Dharmacon; Lafayette, Colorado, USA) solution was prepared by dilution with the corresponding siRNA buffer (Dharmacon), as specified by the manufacturer, of which 120 µl were then added to each 12-well prepared with 12 ml serum-reduced medium. No separate transfection reagent is required for the Dharmacon Accell™-siRNA technology used. In addition to the *Sspn*-targeting siRNA (*Sspn* knockdown), a positive control (PC) directed

against *Gapdh*, a negative control (NC), which consists of four siRNA components with no cellular target for excluding non-sequence-specific effects, and an untreated control (UT) were also included.

After 72 h, all cells were resupplied with medium containing 10 % FBS. After another 72 h (day zero) we started the differentiation of the cells by adding induction medium (DMEM with 10 % FBS, insulin, T3, dexamethasone, indomethacin and IBMX as described above). From day four to eight, the cells were cultured in differentiation medium (DMEM with 10 % FBS, insulin and T3 as described above). RNA extraction on days zero, four and eight and gene expression measurements of *Sspn, Cebpb, Adipoq* and *Pparg* as well as *Rplp0* as the reference gene and *Gapdh* for the evaluation of the NC results were performed as already described.

1.7. Human adipose tissue specific RNA sequencing

Human data were sourced from the cross-sectional cohort (CSC) of the Leipzig Obesity Biobank (LOBB; https://www.helmholtz-munich.de/en/hi-mag/cohort/leipzig-obesity-bio-bank-lobb). The CSC includes 1479 individuals, categorized as either normal/overweight (N = 31; 52 % women; age: 55.8 ± 13.4 years; BMI: 25.7 ± 2.7 kg/m^2) or people with obesity (N = 1448; 71 % women; age: 46.9 ± 11.7 years; BMI: 49.2 ± 8.3 kg/m^2). All participants gave written informed consent before taking part in the study and were informed of the purpose, risks and benefits of the biobank. The study was approved by the ethics committee of the University of Leipzig (#159-12-21052012). For each participant, paired human samples of OVAT and SAT were collected between 2008 and 2018 during elective laparoscopic abdominal surgeries, as previously described (Mardinoglu et al., 2015; Langhardt et al., 2018). Additionally, laboratory measurements of metabolic parameters and body composition were obtained, as detailed in earlier studies (Blüher, 2020; Klöting et al., 2010). The inclusion criteria for the CSC comprised men and women over the age of 18 who underwent elective abdominal surgery. Key exclusion criteria included chronic drug or alcohol abuse, smoking within the 12 months prior to surgery, acute inflammatory diseases, treatment with medications that directly affect adipose tissue, end-stage malignancies, weight loss exceeding three percent in the three months leading up to surgery, uncontrolled thyroid disease, and Cushing's disease.

To generate ribosomal RNA-depleted RNA sequencing data, we employed the SMARTseq protocol (Picelli et al., 2014; Song et al., 2018). The libraries were sequenced as single-end reads on a Novaseq 6000 (Illumina, San Diego, CA, USA) at the Functional Genomics Center Zurich, Switzerland, and analyzed according to the detailed procedure as described elsewhere (Müller et al., 2024).

The preprocessing steps were carried out as previously outlined. In summary, adapter and quality-trimmed reads were aligned to the human reference genome (assembly GRCh38.p13, GENCODE release 32), and gene-level expression quantification was performed using Kallisto v0.48 (Bray et al., 2016). For samples with read counts exceeding 20 million, we down-sampled them to 20 million reads using the R package ezRun v3.14.1 (https://github.com/uzh/ezRun, accessed on April 27, 2023). The data were normalized using a weighted trimmed mean (TMM) of the log expression ratios and adjusted for age, sex, and transcript integrity numbers (TINs).

1.8. Statistical analysis

Spearman's correlation coefficient was employed to assess the relationship between *SSPN* expression and clinical variables, utilizing the psych package (v2.4.6.26) in R (Revelle, 2007). Analyses were conducted in R v4.3.1 (www.R-project.org). Apart from the RNA sequencing data analysis, statistical analysis was conducted using GraphPad Prism 10. Methylation differences, variations in mRNA expression levels and in fluorescence intensity from spectroscopic measurements between treated cells and control cells were analyzed using a two-way ANOVA with multiple comparisons and correction for multiple testing. This analysis incorporated time as a within-subject factor and treatment group as a between-subject factor. P-values <0.05 were considered to be significant.

2. Results

2.1. Correlation of SSPN human adipose tissue mRNA expression with metabolic traits

We investigated the correlation between *Sarcospan (SSPN)* expression and various phenotypic characteristics to explore *SSPN*'s role in lipid metabolism. These analyses were performed separately for visceral and subcutaneous adipose tissues and were additionally stratified by gender to account for potential sex-specific differences. In SAT, *SSPN* expression showed a significant negative correlation with hip circumference ($r = -0.23$, $p < 5 \times 10^{-2}$, $N = 123$), HbA1c levels ($r = -0.09$, $p < 1 \times 10^{-2}$, $N = 790$), fasting plasma glucose (FPG; $r = -0.10$, $p < 1 \times 10^{-3}$, $N = 1327$), and C-reactive protein (CRP; $r = -0.10$, $p < 1 \times 10^{-4}$, $N = 1435$). There were also significant positive correlations with LDL ($r = 0.09$, $p < 1 \times 10^{-2}$, $N = 858$) and HDL ($r = 0.08$, $p < 5 \times 10^{-2}$, $N = 921$) cholesterol levels (Fig. 2). In visceral adipose tissue (VAT), *SSPN* expression was positively correlated with waist circumference ($r = 0.17$, $p < 1 \times 10^{-2}$, $N = 244$) and total body fat ($r = 0.14$, $p = 1 \times 10^{-4}$, $N = 669$, see Supplemental Table 2 for data on all analyzed characteristics). However, after correction for multiple testing only the correlation with

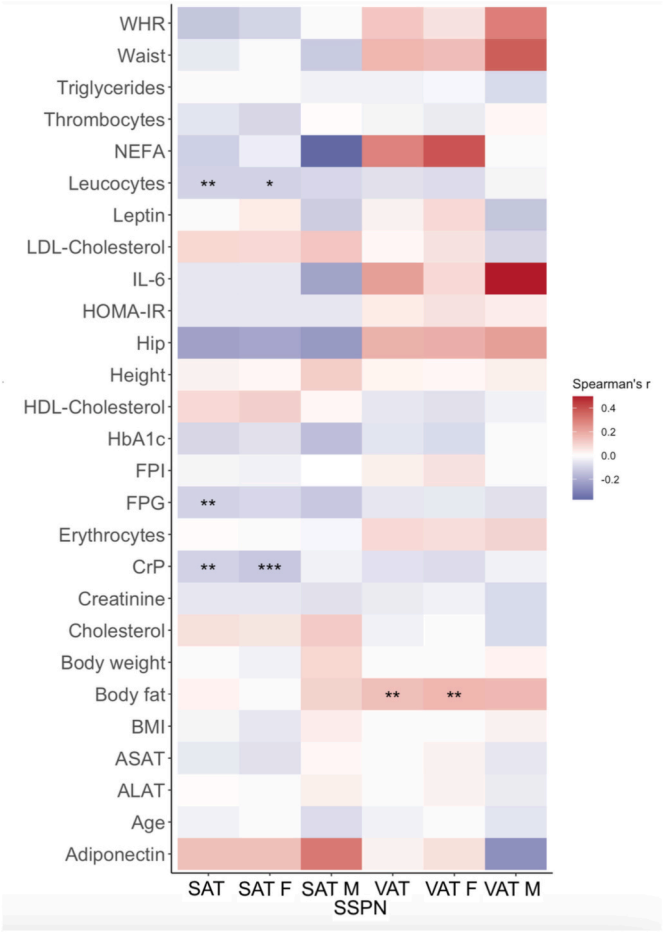

Fig. 2. Correlation analysis of *SSPN* mRNA expression with clinical variables in the Leipzig Obesity Biobank (LOBB) cohort. Heat map shows Spearman correlations between *SSPN* expression and phenotypic traits or blood parameters in subcutaneous (SAT) and visceral (VAT) fat of males (M) and females (F) which are unadjusted for multiple testing. Significance levels are indicated as * <0.05, ** <0.01, *** <0.001 respectively.

FPG and CRP in SAT as well as the correlation with body fat in VAT maintained. In addition, we observed tissue type-specific effect directions for waist and hip measurements. However, findings provided the rationale for more detailed investigations through *in vitro* experiments.

2.2. Effect of increased DNA methylation on Sspn and adipogenic gene expression

The DNA methylation status of four CpG sites within the *Sspn* promoter was analyzed in CRISPR/dCas9-edited cells, referred to as *Sspn* gRNAs, and compared to untreated controls (UT), and controls containing an empty plasmid instead of gRNA, referred to as Plasmid Controls.

The results indicated that methylation in the *Sspn* gRNAs cells was significantly higher than in the Plasmid Controls at all measured time points (all $p < 0.005$, Fig. 3A. Specifically, a substantial increase in methylation of up to 35 % was observed at individual CpG sites in the *Sspn* gRNAs group compared to Plasmid Controls. Importantly, the increased methylation levels remained stable over the entire observation period.

Although mRNA expression analysis revealed only marginal non-significant differences of *Sspn* expression in *Sspn* gRNAs compared to Plasmid Controls throughout differentiation (Fig. 3B), we observed a trend towards reduced *Sspn* expression on days zero and four. In line, mRNA analysis of adipogenic marker genes showed no continuous differences between Plasmid Controls and *Sspn* gRNAs cells (Fig. 4).

Based on this, we replicated our editing experiment in inguinal preadipocytes (see above), which further validated our findings of a stable strong targeted promoter methylation increase with only a trend towards reduced *Sspn* and no remarkable effect on adipogenic gene transcription. The detailed results can be found in the supplements (Supplemental Figs. 1–3).

2.3. Effect of increased DNA methylation on lipid content in adipocytes

Similar to the marginal effects on *Sspn* expression, *Sspn* gRNA treated cells did not show a lower lipid accumulation compared to Plasmid Controls throughout differentiation, although there was a clear increase in lipid content from day zero to day eight (Fig. 3C).

Fluorescence microscopy images allow the assumption of a reduction in lipid storage in *Sspn* gRNA treated cells compared to the controls over the measurement period for epididymal adipocytes (Fig. 5). This was also observable in inguinal adipocytes (see brightfield microscopy of day seven in Supplemental Fig. 4).

2.4. siRNA-induced Sspn knockdown

Based on these findings, we additionally evaluated the impact of *Sspn* knockdown using siRNA on the expression of *Sspn* itself as well as on *Cebpb*, *Adipoq* and *Pparg* in epididymal cells. While results demonstrated a significant reduction of *Sspn* expression (all $p \leq 1 \times 10^{-4}$) in *Sspn* knockdown cells compared to mock-transfected cells until day four of differentiation (Fig. 6A), no significant differences in the expression of adipogenesis markers (*Cebpb*, *Adipoq*, and *Pparg*) were found between *Sspn* knockdown and NC at any time point (Fig. 6B–D).

3. Discussion

Based on the previously reported findings suggesting *SSPN* as a potential candidate gene for BMI and fat distribution, we investigated its role in adipogenesis, particularly focusing on changes in promoter methylation. To this end, we employed both *Sspn* knockdown using siRNA and CRISPR/dCas9-induced hypermethylation in a mouse cell model, to explore whether the postulated influence of *Sspn* on adipogenesis was epigenetically mediated.

Using the αGCN4-coupled CRISPR/dCas9-SunTag-DNMT3a system, we were able to achieve stable hypermethylation in murine preadipocytes over several days, indicating that any conceivable gradual degradation of the plasmids likely did not affect our experimental setup. The resulting decrease in *Sspn* expression was recognizable as a trend but did not reach statistical significance. Although editing of the target CpG sites increased methylation levels significantly, it is possible that DNA methylation editing in the area of our target sequence, even if we ascribe it an involvement in the regulation of *Sspn* expression, cannot alone influence mRNA levels. It is of note however, that even with minimal differences in promoter methylation (1.72 ± 1.3 % in SAT and 1.89 ± 1.9 % in OVAT) in human samples, at the genomic position which corresponds to our murine target sequence, Keller et al. (2018) showed significant correlations with WHR and body fat, suggesting that the level of methylation achieved in the present study should be sufficient to elicit detectable effects – yet findings based on human data cannot readily be transferred to the animal model.

Overall, the assessment of adipogenesis through various methods did not yield entirely consistent conclusions. While microscopy suggested an editing effect on lipid storage, which was not confirmed by fluorescence spectroscopy and expression of adipogenic genes, other authors were able to show differences in gene expression of adipogenesis markers in mouse adipose tissue between lipogenic state (caused by high-energy, high-fat diet) and controls (Illesca et al., 2019, 2020). Because the effects seen in fluorescence microscopy could not be objectified by quantification, we view these observations with caution.

Another factor that may have obscured the influence of *Sspn* on adipogenesis is the possibility of off-target effects. Even though Pflueger

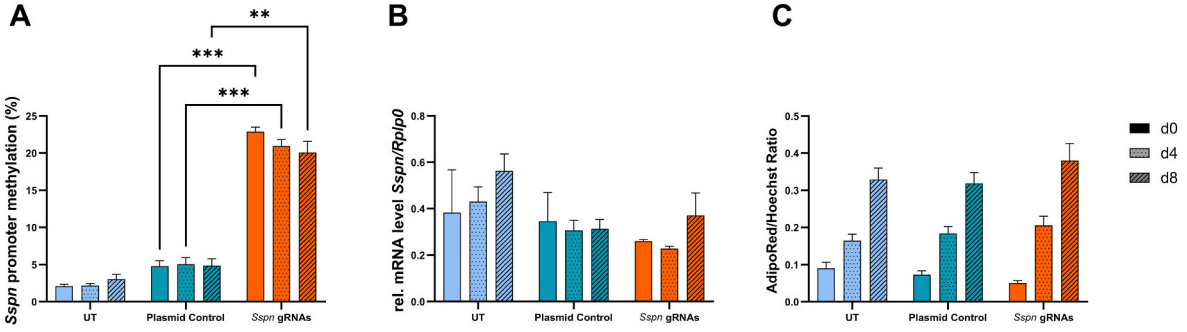

Fig. 3. Analysis of *in vitro Sspn* promoter methylation, *Sspn* gene expression and fluorescence spectroscopy measurements. Bar plots show *Sspn* promoter methylation levels (A), *Sspn* mRNA expression levels relative to the housekeeping gene *Rplp0* (B) and intensity of fluorescence signal in AdipoRed/Hoechst stained cells (C) in epididymal adipocytes. Data are shown for days zero (d0), four (d4) and eight (d8) of the differentiation in UT, Plasmid Controls and *Sspn* gRNAs with mean and SEM. Analyzed using two-way ANOVA with correction for multiple testing. Significance levels are indicated as * <0.05, ** <0.01, *** <0.001 respectively. N = 3.

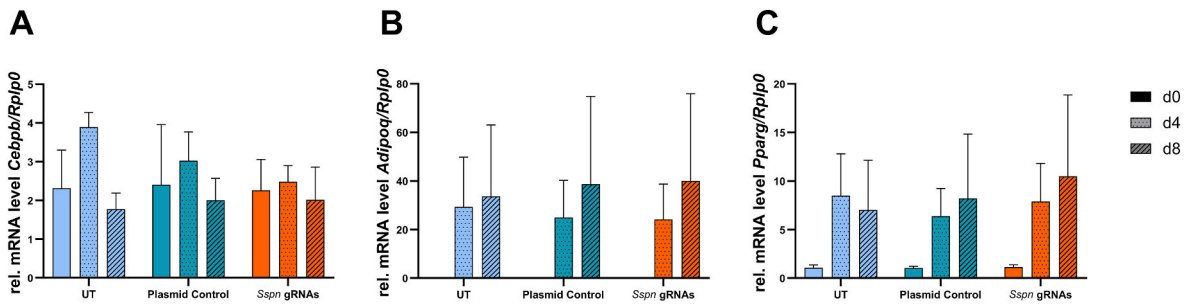

Fig. 4. Gene expression of adipogenesis markers. Bar plots show relative mRNA levels to *Rplp0* as the housekeeping gene for *Cebpb*, *Adipoq* and *Pparg* in epididymal cells on days zero (d0), four (d4) and eight (d8) of the differentiation in UT, Plasmid Controls and *Sspn* gRNAs with mean and SEM. Analyzed using two-way ANOVA with correction for multiple testing. Significance levels are indicated as * <0.05, ** <0.01, *** <0.001 respectively. N = 3.

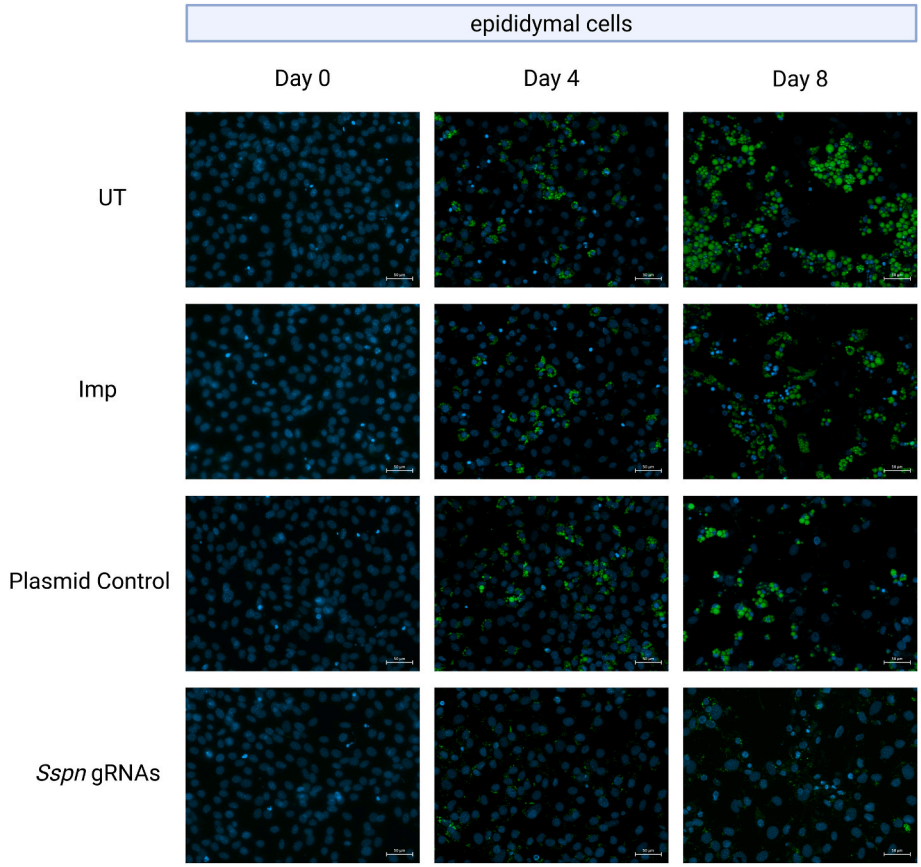

Fig. 5. Fluorescence microscopy. Fluorescence images sections of epididymal adipocytes on days zero, four and eight of the differentiation. Blue: Nuclei stained with Hoechst. Green: Lipids stained with AdipoRed. Scale bar = 50 μm. Images were arranged using Biorender.com.

et al. (2018) demonstrated that the αGCN4-coupled CRISPR/dCas9-SunTag-DNMT3a system induced negligible off-target effects in HeLa cells, we cannot rule out that off-target methylation may have limited the magnitude of the expected effect. The observation that the differences between Plasmid Controls and *Sspn* gRNAs were not as large as the differences between UT and *Sspn* gRNAs, for example, also indicates that the presence of dCas9 or DNMT3a in the cell per se could also have effects that are to be distinguished from the methylation effects at the *Sspn* promoter.

In a previous series of experiments with paired SAT and OVAT samples, depot-specific correlations with metabolic traits have been shown (Keller et al., 2018). As such, correlations between *SSPN* promoter methylation and hip circumference, glucose measurements or maximum adipocyte size were only reported in SAT (Keller et al., 2018). Despite the loss of statistical significance after correction for multiple testing, in our large-scale analysis of data from the LOBB we observed that the direction of the correlation between the tissue types was different for waist and hip, which supports the hypothesis that *SSPN* may play a role in the regulation of lipid metabolism. The data suggest a potential differential involvement of *SSPN* in various fat depots, emphasizing the need to distinguish between subcutaneous and visceral fat when evaluating *SSPN*'s functional significance. We performed the CRISPR/dCas9-mediated hypermethylation in both epididymal preadipocytes, which correspond to OVAT, and inguinal preadipocytes (see Supplements), which correspond to SAT, to address eventual fat depot specific effects. However, findings in epididymal and inguinal cells were comparable in all our experiments.

In addition, neither the epigenetic editing nor the siRNA-knockdown showed signs of lipodystrophy as previously described by Groh et al. in β-sarcoglycan knockout mice lacking both Sspn and the sarcoglycans

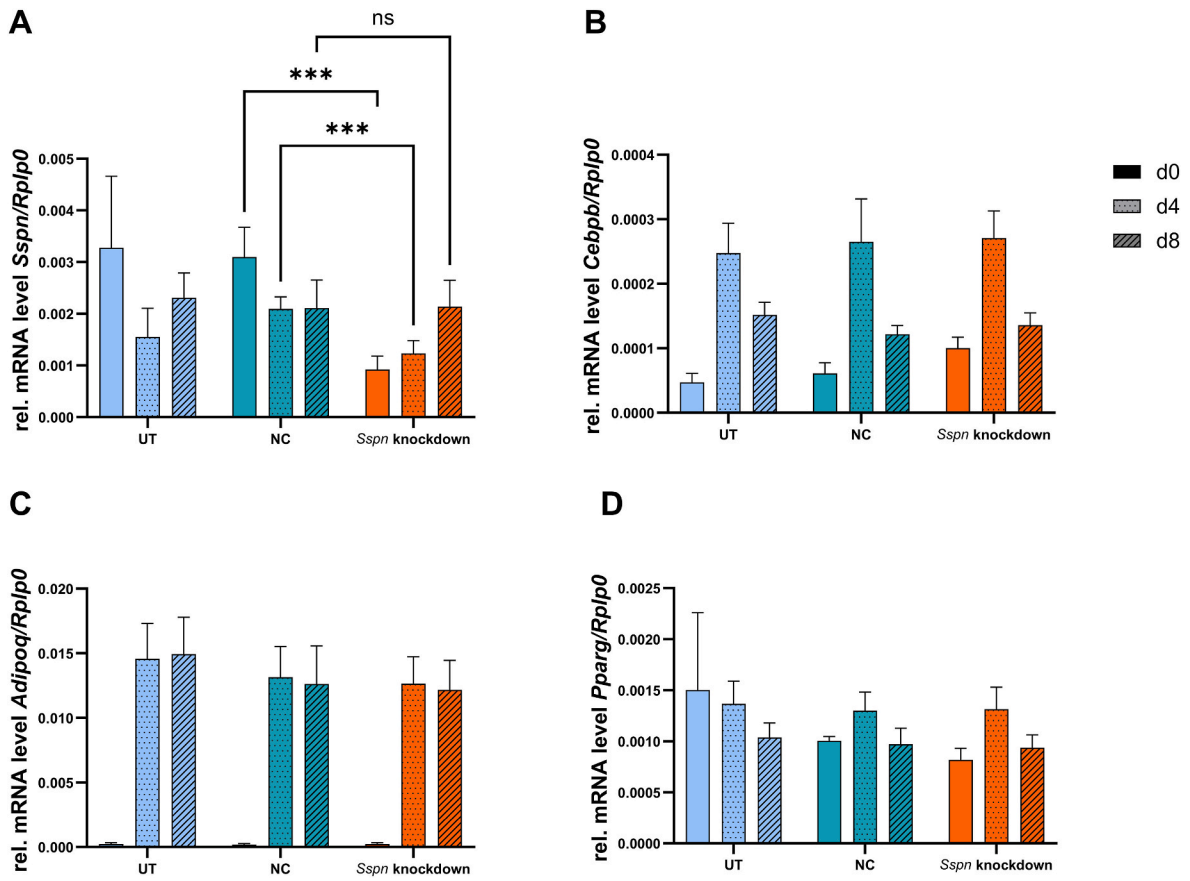

Fig. 6. Gene expression of *Sspn* and adipogenesis markers after siRNA knockdown of *Sspn*. Bar plots show relative mRNA levels to *Rplp0* as the housekeeping gene for *Sspn* (A) *Cebpb (B)*, *Adipoq (C)* and *Pparg* (D) in epididymal cells on days zero (d0), four (d4) and eight (d8) of the differentiation in UT, NC and *Sspn* knockdown cells with mean and SEM. Analyzed using two-way ANOVA with correction for multiple testing. Significance levels are indicated as * <0.05, ** <0.01, *** <0.001 respectively. N = 3.

(Groh et al., 2009), at least as far as these can be assessed in a 2D cell culture model. However, we are aware that future experiments have to investigate the effects on protein levels, especially since public data indicate that SSPN protein is upregulated during differentiation to mature adipocytes (Zhong et al., 2025). It is therefore reasonable to assume that the loss of a whole series of sarcoglycans has more far-reaching consequences than just the downregulation of *Sspn* alone. Nonetheless, the study by Groh et al. emphasizes the need for further investigation of *SSPN* as an important player in adipose tissue. To better understand the role of *SSPN*, a possible *SSPN* upregulation in adipose tissue should also be considered.

Accordingly, it is necessary to keep in mind that SSPN is a transmembrane protein whose function is decisively determined by its interaction with the extracellular matrix. It is therefore conceivable that potential effects of *SSPN* editing may not be detectable in a 2D cell culture model, which can only partially mimic the conditions in adipose tissue. The absence of extracellular matrix between the individual adipocytes as well as other cell types or tissue hormones, to name just a few influencing factors, represent weaknesses of the 2D cell culture model. It is quite possible that the SSPN protein could exert its full function only in a 3D culture model or in an *in vivo* experiment, which might reveal differences between *SSPN* edits and controls regarding adipocyte storage. That the influence of *SSPN* on adipogenesis may be mediated by its mode of action as a matrix protein is also supported by the finding of Soták et al. (2022) showing that the quantity of extracellular matrix differs between obese and normal weight individuals. Interestingly, in this study, lean individuals showed higher amounts and gene expression of extracellular matrix components, whereas in the cohort of Keller et al., the matrix protein *SSPN* was associated with adverse clinical parameters connected with obesity (Keller et al., 2018).

Nevertheless, our correlation data from the human LOBB cohort showed a clear association between *SSPN* gene expression and various clinical features describing fat distribution. The fact that we could not achieve direct effects on adipogenesis by epigenetic downregulation of the *Sspn* promoter does not diminish the importance of *SSPN* as a candidate gene for obesity research. Rather, the significant correlations observed in both visceral and subcutaneous adipose tissue highlight the potential to gain further insights into its effects on adipogenesis using an optimized model that accounts for *SSPN's* role as an extracellular matrix component. This could ultimately support the development of *in vivo* models and future applications in targeted, tissue-specific epigenetic gene regulation in humans.

In summary, our study proved that targeted DNA methylation editing of the *Sspn* promoter leads to a stable hypermethylation in adipocytes but has only marginal effects on *Sspn* expression and adipogenesis. However, large-scale phenotypic associations of depot-specific *SSPN* expression with parameters of fat distribution and glucose homeostasis still make it a promising candidate in adipose tissue biology.

CRediT authorship contribution statement

Katharina Anastasia Dinter: Writing – original draft, Visualization, Investigation, Data curation. **Samantha Aurich:** Validation, Data curation. **Luise Müller:** Writing – review & editing, Visualization, Data curation. **Adhideb Ghosh:** Data curation. **Falko Noé:** Data curation. **Christian Wolfrum:** Data curation. **Matthias Blüher:** Writing – review & editing, Funding acquisition. **Anne Hoffmann:** Writing – review & editing, Visualization, Data curation. **Peter Kovacs:** Writing – review &

editing, Supervision. **Maria Keller:** Writing – review & editing, Supervision, Project administration, Funding acquisition, Conceptualization.

Disclosure statement

MB received honoraria as a consultant and speaker from Amgen, AstraZeneca, Bayer, Boehringer Ingelheim, Daiichi-Sankyo, Lilly, Novo Nordisk, Novartis, and Sanofi. All other authors have nothing to disclose.

Funding

This work was supported by Deutsches Zentrum für Diabetesforschung (DZD, Grant: 82DZD06D03 to PK, Grant: 82DZD00601 to MB) and the German Diabetes Society to MK. Further support was obtained from Deutsche Forschungsgemeinschaft (DFG) for a Collaborative Research Center (CRC 1052/2, project number 209933838): "Obesity mechanisms" (B1 to MB, B3 to PK and KAD).

Declaration of competing interest

The authors declare the following financial interests/personal relationships which may be considered as potential competing interests: Matthias Bluher reports a relationship with Amgen, AstraZeneca, Bayer, Boehringer Ingelheim, Daiichi-Sankyo, Lilly, Novo Nordisk, Novartis, and Sanofi that includes: consulting or advisory and speaking and lecture fees. If there are other authors, they declare that they have no known competing financial interests or personal relationships that could have appeared to influence the work reported in this paper.

Acknowledgements

Prof. Klein and Dr. Perwitz from the Medical University of Lübeck kindly provided immortalized epididymal and inguinal murine preadipocytes for this work. We thank Wenfei Sun and Hua Dong for supporting human adipose tissue RNA sequencing of the LOBB, the Core Facility for DNA technologies of Knut Krohn from the University of Leipzig for the collaboration on DNA sequencing as well as the Core Unit Fluorescence Technologies of Kathrin Jäger from the University of Leipzig for their assistance with cell sorting. We would also like to acknowledge Ines Müller, Claudia Ruffert and Beate Gutsmann for their great guidance and support in the laboratory.

Appendix ASupplementary data

Supplementary data to this article can be found online at https://doi.org/10.1016/j.mce.2025.112602.

Data availability

The data that support the findings of this study are available in the Materials and Methods, Results, and Supplemental Material of this article. The human RNA-sequencing data from the LOBB are not deposited in a public repository due to patient consent restrictions but are available on request from Matthias Blüher.

References

Blüher, M., 2020. Metabolically healthy obesity. Endocr. Rev. 41.
Bray, N.L., Pimentel, H., Melsted, P., Pachter, L., 2016. Near-optimal probabilistic RNA-seq quantification. Nat. Biotechnol. 34, 525–527.
Ceco, E., McNally, E.M., 2013. Modifying muscular dystrophy through transforming growth factor-β. FEBS J. 280, 4198–4209.
Concordet, J.-P., Haeussler, M., 2018. CRISPOR: intuitive guide selection for CRISPR/Cas9 genome editing experiments and screens. Nucleic Acids Res. 46, W242–W245.
Crosbie, R.H., Heighway, J., Venzke, D.P., Lee, J.C., Campbell, K.P., 1997. Sarcospan, the 25-kDa transmembrane component of the dystrophin-glycoprotein complex. J. Biol. Chem. 272, 31221–31224.
Groh, S., Zong, H., Goddeeris, M.M., Lebakken, C.S., Venzke, D., Pessin, J.E., Campbell, K.P., 2009. Sarcoglycan complex: implications for metabolic defects in muscular dystrophies. J. Biol. Chem. 284, 19178–19182.
Heid, I.M., Jackson, A.U., Randall, J.C., Winkler, T.W., Qi, L., Steinthorsdottir, V., Thorleifsson, G., Zillikens, M.C., Speliotes, E.K., Mägi, R., Workalemahu, T., White, C.C., Bouatia-Naji, N., Harris, T.B., Berndt, S.I., Ingelsson, E., Willer, C.J., Weedon, M.N., Luan, J.'a., Vedantam, S., Esko, T., Kilpeläinen, T.O., Kutalik, Z., Li, S., Monda, K.L., Dixon, A.L., Holmes, C.C., Kaplan, L.M., Liang, L., Min, J.L., Moffatt, M.F., Molony, C., Nicholson, G., Schadt, E.E., Zondervan, K.T., Feitosa, M.F., Ferreira, T., Lango Allen, H., Weyant, R.J., Wheeler, E., Wood, A.R., Estrada, K., Goddard, M.E., Lettre, G., Mangino, M., Nyholt, D.R., Purcell, S., Smith, A.V., Visscher, P.M., Yang, J., McCarroll, S.A., Nemesh, J., Voight, B.F., Absher, D., Amin, N., Aspelund, T., Coin, L., Glazer, N.L., Hayward, C., Heard-Costa, N.L., Hottenga, J.-J., Johansson, A., Johnson, T., Kaakinen, M., Kapur, K., Ketkar, S., Knowles, J.W., Kraft, P., Kraja, A.T., Lamina, C., Leitzmann, M.F., McKnight, B., Morris, A.P., Ong, K.K., Perry, J.R.B., Peters, M.J., Polasek, O., Prokopenko, I., Rayner, N.W., Ripatti, S., Rivadeneira, F., Robertson, N.R., Sanna, S., Sovio, U., Surakka, I., Teumer, A., van Wingerden, S., Vitart, V., Zhao, J.H., Cavalcanti-Proença, C., Chines, P.S., Fisher, E., Kulzer, J.R., Lecoeur, C., Narisu, N., Sandholt, C., Scott, L.J., Silander, K., Stark, K., Tammesoo, M.-L., Teslovich, T.M., Timpson, N.J., Watanabe, R.M., Welch, R., Chasman, D.I., Cooper, M.N., Jansson, J.-O., Kettunen, J., Lawrence, R.W., Pellikka, N., Perola, M., Vandenput, L., Alavere, H., Almgren, P., Atwood, L.D., Bennett, A.J., Biffar, R., Bonnycastle, L.L., Bornstein, S.R., Buchanan, T.A., Campbell, H., Day, I.N.M., Dei, M., Dörr, M., Elliott, P., Erdos, M.R., Eriksson, J.G., Freimer, N.B., Fu, M., Gaget, S., Geus, E.J.C., Gjesing, A.P., Grallert, H., Grässler, J., Groves, C.J., Guiducci, C., Hartikainen, A.-L., Hassanali, N., Havulinna, A.S., Herzig, K.-H., Hicks, A.A., Hui, J., Igl, W., Jousilahti, P., Jula, A., Kajantie, E., Kinnunen, L., Kolcic, I., Koskinen, S., Kovacs, P., Kroemer, H.K., Krzelj, V., Kuusisto, J., Kvaloy, K., Laitinen, J., Lantieri, O., Lathrop, G.M., Lokki, M.-L., Luben, R.N., Ludwig, B., McArdle, W.L., McCarthy, A., Morken, M.A., Nelis, M., Neville, M.J., Paré, G., Parker, A.N., Peden, J.F., Pichler, I., Pietiläinen, K.H., Platou, C.G.P., Pouta, A., Ridderstråle, M., Samani, N.J., Saramies, J., Sinisalo, J., Smit, J.H., Strawbridge, R.J., Stringham, H.M., Swift, A.J., Teder-Laving, M., Thomson, B., Usala, G., van Meurs, J.B.J., van Ommen, G.-J., Vatin, V., Volpato, C. B., Wallaschofski, H., Walters, G.B., Widen, E., Wild, S.H., Willemsen, G., Witte, D. R., Zgaga, L., Zitting, P., Beilby, J.P., James, A.L., Kähönen, M., Lehtimäki, T., Nieminen, M.S., Ohlsson, C., Palmer, L.J., Raitakari, O., Ridker, P.M., Stumvoll, M., Tönjes, A., Viikari, J., Balkau, B., Ben-Shlomo, Y., Bergman, R.N., Boeing, H., Smith, G.D., Ebrahim, S., Froguel, P., Hansen, T., Hengstenberg, C., Hveem, K., Isomaa, B., Jørgensen, T., Karpe, F., Khaw, K.-T., Laakso, M., Lawlor, D.A., Marre, M., Meitinger, T., Metspalu, A., Midthjell, K., Pedersen, O., Salomaa, V., Schwarz, P.E.H., Tuomi, T., Tuomilehto, J., Valle, T.T., Wareham, N.J., Arnold, A.M., Beckmann, J.S., Bergmann, S., Boerwinkle, E., Boomsma, D.I., Caulfield, M.J., Collins, F.S., Eiriksdottir, G., Gudnason, V., Gyllensten, U., Hamsten, A., Hattersley, A.T., Hofman, A., Hu, F.B., Illig, T., Iribarren, C., Jarvelin, M.-R., Kao, W. H.L., Kaprio, J., Launer, L.J., Munroe, P.B., Oostra, B., Penninx, B.W., Pramstaller, P. P., Psaty, B.M., Quertermous, T., Rissanen, A., Rudan, I., Shuldiner, A.R., Soranzo, N., Spector, T.D., Syvanen, A.-C., Uda, M., Uitterlinden, A., Völzke, H., Vollenweider, P., Wilson, J.F., Witteman, J.C., Wright, A.F., Abecasis, G.R., Boehnke, M., Borecki, I.B., Deloukas, P., Frayling, T.M., Groop, L.C., Haritunians, T., Hunter, D.J., Kaplan, R.C., North, K.E., O'Connell, J.R., Peltonen, L., Schlessinger, D., Strachan, D.P., Hirschhorn, J.N., Assimes, T.L., Wichmann, H.-E., Thorsteinsdottir, U., van Duijn, C.M., Stefansson, K., Cupples, L.A., Loos, R.J.F., Barroso, I., McCarthy, M.I., Fox, C.S., Mohlke, K.L., Lindgren, C.M., 2010. Meta-analysis identifies 13 new loci associated with waist-hip ratio and reveals sexual dimorphism in the genetic basis of fat distribution. Nat. Genet. 42, 949–960.
Hiuge-Shimizu, A., Kishida, K., Funahashi, T., Ishizaka, Y., Oka, R., Okada, M., Suzuki, S., Takaya, N., Nakagawa, T., Fukui, T., Fukuda, H., Watanabe, N., Yoshizumi, T., Nakamura, T., Matsuzawa, Y., Yamakado, M., Shimomura, I., 2012. Absolute value of visceral fat area measured on computed tomography scans and obesity-related cardiovascular risk factors in large-scale Japanese general population (the VACATION-J study). Ann. Med. 44, 82–92.
Illesca, P., Valenzuela, R., Espinosa, A., Echeverría, F., Soto-Alarcon, S., Ortiz, M., Videla, L.A., 2019. Hydroxytyrosol supplementation ameliorates the metabolic disturbances in white adipose tissue from mice fed a high-fat diet through recovery of transcription factors Nrf2, SREBP-1c, PPAR-γ and NF-κB. Biomed. Pharmacother. = Biomedecine; pharmacotherapie 109, 2472–2481.
Illesca, P., Valenzuela, R., Espinosa, A., Echeverría, F., Soto-Alarcón, S., Ortiz, M., Campos, C., Vargas, R., Videla, L.A., 2020. The metabolic dysfunction of white adipose tissue induced in mice by a high-fat diet is abrogated by co-administration of docosahexaenoic acid and hydroxytyrosol. Food Funct. 11, 9086–9102.
Keller, M., Hopp, L., Liu, X., Wohland, T., Rohde, K., Cancello, R., Klös, M., Bacos, K., Kern, M., Eichelmann, F., Dietrich, A., Schön, M.R., Gärtner, D., Lohmann, T., Dreßler, M., Stumvoll, M., Kovacs, P., DiBlasio, A.-M., Ling, C., Binder, H., Blüher, M., Böttcher, Y., 2017. Genome-wide DNA promoter methylation and transcriptome analysis in human adipose tissue unravels novel candidate genes for obesity. Mol. Metabol. 6, 86–100.
Keller, M., Klös, M., Rohde, K., Krüger, J., Kurze, T., Dietrich, A., Schön, M.R., Gärtner, D., Lohmann, T., Dreßler, M., Stumvoll, M., Blüher, M., Kovacs, P., Böttcher, Y., 2018. DNA methylation of SSPN is linked to adipose tissue distribution and glucose metabolism. FASEB J. Offic. Pub. Federat. Am. Soc. Experim. Biol. fj201800528R.
Klöting, N., Fasshauer, M., Dietrich, A., Kovacs, P., Schön, M.R., Kern, M., Stumvoll, M., Blüher, M., 2010. Insulin-sensitive obesity. Am. J. Physiol. Endocrinol. Metabol. 299, E506–E515.

Kovsan, J., Osnis, A., Maissel, A., Mazor, L., Tarnovscki, T., Hollander, L., Ovadia, S., Meier, B., Klein, J., Bashan, N., Rudich, A., 2009. Depot-specific adipocyte cell lines reveal differential drug-induced responses of white adipocytes–relevance for partial lipodystrophy. Am. J. Physiol. Endocrinol. Metabol. 296, E315–E322.
Kuhn, R.M., Haussler, D., Kent, W.J., 2013. The UCSC genome browser and associated tools. Briefings Bioinf. 14, 144–161.
Langhardt, J., Flehmig, G., Klöting, N., Lehmann, S., Ebert, T., Kern, M., Schön, M.R., Gärtner, D., Lohmann, T., Dressler, M., Fasshauer, M., Kovacs, P., Stumvoll, M., Dietrich, A., Blüher, M., 2018. Effects of weight loss on glutathione peroxidase 3 serum concentrations and adipose tissue expression in human obesity. Obes. Facts 11, 475–490.
Liu, C.-T., Monda, K.L., Taylor, K.C., Lange, L., Demerath, E.W., Palmas, W., Wojczynski, M.K., Ellis, J.C., Vitolins, M.Z., Liu, S., Papanicolaou, G.J., Irvin, M.R., Xue, L., Griffin, P.J., Nalls, M.A., Adeyemo, A., Liu, J., Li, G., Ruiz-Narvaez, E.A., Chen, W.-M., Chen, F., Henderson, B.E., Millikan, R.C., Ambrosone, C.B., Strom, S.S., Guo, X., Andrews, J.S., Sun, Y.V., Mosley, T.H., Yanek, L.R., Shriner, D., Haritunians, T., Rotter, J.I., Speliotes, E.K., Smith, M., Rosenberg, L., Mychaleckyj, J., Nayak, U., Spruill, I., Garvey, W.T., Pettaway, C., Nyante, S., Bandera, E.V., Britton, A.F., Zonderman, A.B., Rasmussen-Torvik, L.J., Chen, Y.-D.I., Ding, J., Lohman, K., Kritchevsky, S.B., Zhao, W., Peyser, P.A., Kardia, S.L.R., Kabagambe, E., Broeckel, U., Chen, G., Zhou, J., Wassertheil-Smoller, S., Neuhouser, M.L., Rampersaud, E., Psaty, B., Kooperberg, C., Manson, J.E., Kuller, L. H., Ochs-Balcom, H.M., Johnson, K.C., Sucheston, L., Ordovas, J.M., Palmer, J.R., Haiman, C.A., McKnight, B., Howard, B.V., Becker, D.M., Bielak, L.F., Liu, Y., Allison, M.A., Grant, S.F.A., Burke, G.L., Patel, S.R., Schreiner, P.J., Borecki, I.B., Evans, M.K., Taylor, H., Sale, M.M., Howard, V., Carlson, C.S., Rotimi, C.N., Cushman, M., Harris, T.B., Reiner, A.P., Cupples, L.A., North, K.E., Fox, C.S., 2013. Genome-wide association of body fat distribution in African ancestry populations suggests new loci. PLoS Genet. 9, e1003681.
Mardinoglu, A., Heiker, J.T., Gärtner, D., Björnson, E., Schön, M.R., Flehmig, G., Klöting, N., Krohn, K., Fasshauer, M., Stumvoll, M., Nielsen, J., Blüher, M., 2015. Extensive weight loss reveals distinct gene expression changes in human subcutaneous and visceral adipose tissue. Sci. Rep. 5, 14841.
Marshall, J.L., Crosbie-Watson, R.H., 2013. Sarcospan: a small protein with large potential for Duchenne muscular dystrophy. Skeletal Muscle 3, 1.
Marshall, J.L., Holmberg, J., Chou, E., Ocampo, A.C., Oh, J., Lee, J., Peter, A.K., Martin, P.T., Crosbie-Watson, R.H., 2012a. Sarcospan-dependent Akt activation is required for utrophin expression and muscle regeneration. J. Cell Biol. 197, 1009–1027.
Marshall, J.L., Chou, E., Oh, J., Kwok, A., Burkin, D.J., Crosbie-Watson, R.H., 2012b. Dystrophin and utrophin expression require sarcospan: loss of α7 integrin exacerbates a newly discovered muscle phenotype in sarcospan-null mice. Hum. Mol. Genet. 21, 4378–4393.
Müller, L., Hoffmann, A., Bernhart, S.H., Ghosh, A., Zhong, J., Hagemann, T., Sun, W., Dong, H., Noé, F., Wolfrum, C., Dietrich, A., Stumvoll, M., Massier, L., Blüher, M., Kovacs, P., Chakaroun, R., Keller, M., 2024. Blood methylation pattern reflects epigenetic remodelling in adipose tissue after bariatric surgery. EBioMedicine 106, 105242.
Neeland, I.J., Turer, A.T., Ayers, C.R., Powell-Wiley, T.M., Vega, G.L., Farzaneh-Far, R., Grundy, S.M., Khera, A., McGuire, D.K., Lemos, J. A. de, 2012. Dysfunctional adiposity and the risk of prediabetes and type 2 diabetes in obese adults. JAMA 308, 1150–1159.
Neeland, I.J., Ayers, C.R., Rohatgi, A.K., Turer, A.T., Berry, J.D., Das, S.R., Vega, G.L., Khera, A., McGuire, D.K., Grundy, S.M., Lemos, J. A. de, 2013. Associations of visceral and abdominal subcutaneous adipose tissue with markers of cardiac and metabolic risk in obese adults. Obesity (Silver Spring, Md.) 21, E439–E447.
Neeland, I.J., Turer, A.T., Ayers, C.R., Berry, J.D., Rohatgi, A., Das, S.R., Khera, A., Vega, G.L., McGuire, D.K., Grundy, S.M., Lemos, J. A. de, 2015. Body fat distribution and incident cardiovascular disease in obese adults. J. Am. Coll. Cardiol. 65, 2150–2151.
Peter, A.K., Marshall, J.L., Crosbie, R.H., 2008. Sarcospan reduces dystrophic pathology: stabilization of the utrophin-glycoprotein complex. J. Cell Biol. 183, 419–427.
Pfaffl, M.W., 2001. A new mathematical model for relative quantification in real-time RT-PCR. Nucleic Acids Res. 29, e45.
Pflueger, C., Tan, D., Swain, T., Nguyen, T., Pflueger, J., Nefzger, C., Polo, J.M., Ford, E., Lister, R., 2018. A modular dCas9-SunTag DNMT3A epigenome editing system overcomes pervasive off-target activity of direct fusion dCas9-DNMT3A constructs. Genome Res. 28, 1193–1206.
Picelli, S., Faridani, O.R., Björklund, A.K., Winberg, G., Sagasser, S., Sandberg, R., 2014. Full-length RNA-seq from single cells using Smart-seq2. Nat. Protoc. 9, 171–181.
Revelle, W., 2007. CRAN: Contributed Packages.
Rohde, K., Keller, M., La Cour Poulsen, L., Blüher, M., Kovacs, P., Böttcher, Y., 2019. Genetics and epigenetics in obesity. Metab., Clin. Exp. 92, 37–50.
Shungin, D., Winkler, T.W., Croteau-Chonka, D.C., Ferreira, T., Locke, A.E., Mägi, R., Strawbridge, R.J., Pers, T.H., Fischer, K., Justice, A.E., Workalemahu, T., Wu, J.M. W., Buchkovich, M.L., Heard-Costa, N.L., Roman, T.S., Drong, A.W., Song, C., Gustafsson, S., Day, F.R., Esko, T., Fall, T., Kutalik, Z., Luan, J.'a., Randall, J.C., Scherag, A., Vedantam, S., Wood, A.R., Chen, J., Fehrmann, R., Karjalainen, J., Kahali, B., Liu, C.-T., Schmidt, E.M., Absher, D., Amin, N., Anderson, D., Beekman, M., Bragg-Gresham, J.L., Buyske, S., Demirkan, A., Ehret, G.B., Feitosa, M. F., Goel, A., Jackson, A.U., Johnson, T., Kleber, M.E., Kristiansson, K., Mangino, M., Leach, I.M., Medina-Gomez, C., Palmer, C.D., Pasko, D., Pechlivanis, S., Peters, M.J., Prokopenko, I., Stančáková, A., Sung, Y.J., Tanaka, T., Teumer, A., van Vliet-Ostaptchouk, J.V., Yengo, L., Zhang, W., Albrecht, E., Ärnlöv, J., Arscott, G.M., Bandinelli, S., Barrett, A., Bellis, C., Bennett, A.J., Berne, C., Blüher, M., Böhringer, S., Bonnet, F., Böttcher, Y., Bruinenberg, M., Carba, D.B., Caspersen, I.H., Clarke, R., Daw, E.W., Deelen, J., Deelman, E., Delgado, G., Doney, A.S., Eklund, N., Erdos, M.R., Estrada, K., Eury, E., Friedrich, N., Garcia, M.E., Giedraitis, V., Gigante, B., Go, A.S., Golay, A., Grallert, H., Grammer, T.B., Gräßler, J., Grewal, J., Groves, C.J., Haller, T., Hallmans, G., Hartman, C.A., Hassinen, M., Hayward, C., Heikkilä, K., Herzig, K.-H., Helmer, Q., Hillege, H.L., Holmen, O., Hunt, S.C., Isaacs, A., Ittermann, T., James, A.L., Johansson, I., Juliusdottir, T., Kalafati, I.-P., Kinnunen, L., Koenig, W., Kooner, I.K., Kratzer, W., Lamina, C., Leander, K., Lee, N. R., Lichtner, P., Lind, L., Lindström, J., Lobbens, S., Lorentzon, M., Mach, F., Magnusson, P.K., Mahajan, A., McArdle, W.L., Menni, C., Merger, S., Mihailov, E., Milani, L., Mills, R., Moayyeri, A., Monda, K.L., Mooijaart, S.P., Mühleisen, T.W., Mulas, A., Müller, G., Müller-Nurasyid, M., Nagaraja, R., Nalls, M.A., Narisu, N., Glorioso, N., Nolte, I.M., Olden, M., Rayner, N.W., Renstrom, F., Ried, J.S., Robertson, N.R., Rose, L.M., Sanna, S., Scharnagl, H., Scholtens, S., Sennblad, B., Seufferlein, T., Sitlani, C.M., Smith, A.V., Stirrups, K., Stringham, H.M., Sundström, J., Swertz, M.A., Swift, A.J., Syvänen, A.-C., Tayo, B.O., Thorand, B., Thorleifsson, G., Tomaschitz, A., Troffa, C., van Oort, F.V., Verweij, N., Vonk, J.M., Waite, L.L., Wennauer, R., Wilsgaard, T., Wojczynski, M.K., Wong, A., Zhang, Q., Zhao, J.H., Brennan, E.P., Choi, M., Eriksson, P., Folkersen, L., Franco-Cereceda, A., Gharavi, A.G., Hedman, Å.K., Hivert, M.-F., Huang, J., Kanoni, S., Karpe, F., Keildson, S., Kiryluk, K., Liang, L., Lifton, R.P., Ma, B., McKnight, A.J., McPherson, R., Metspalu, A., Min, J.L., Moffatt, M.F., Montgomery, G.W., Murabito, J.M., Nicholson, G., Nyholt, D.R., Olsson, C., Perry, J.R., Reinmaa, E., Salem, R.M., Sandholm, N., Schadt, E.E., Scott, R.A., Stolk, L., Vallejo, E.E., Westra, H.-J., Zondervan, K.T., Amouyel, P., Arveiler, D., Bakker, S.J., Beilby, J., Bergman, R.N., Blangero, J., Brown, M.J., Burnier, M., Campbell, H., Chakravarti, A., Chines, P.S., Claudi-Boehm, S., Collins, F.S., Crawford, D.C., Danesh, J., Faire, U. de, Geus, E. J. de, Dörr, M., Erbel, R., Eriksson, J.G., Farrall, M., Ferrannini, E., Ferrières, J., Forouhi, N.G., Forrester, T., Franco, O.H., Gansevoort, R.T., Gieger, C., Gudnason, V., Haiman, C.A., Harris, T.B., Hattersley, A.T., Heliövaara, M., Hicks, A. A., Hingorani, A.D., Hoffmann, W., Hofman, A., Homuth, G., Humphries, S.E., Hyppönen, E., Illig, T., Jarvelin, M.-R., Johansen, B., Jousilahti, P., Jula, A.M., Kaprio, J., Kee, F., Keinanen-Kiukaanniemi, S.M., Kooner, J.S., Kooperberg, C., Kovacs, P., Kraja, A.T., Kumari, M., Kuulasmaa, K., Kuusisto, J., Lakka, T.A., Langenberg, C., Le Marchand, L., Lehtimäki, T., Lyssenko, V., Männistö, S., Marette, A., Matise, T.C., McKenzie, C.A., McKnight, B., Musk, A.W., Möhlenkamp, S., Morris, A.D., Nelis, M., Ohlsson, C., Oldehinkel, A.J., Ong, K.K., Palmer, L.J., Penninx, B.W., Peters, A., Pramstaller, P.P., Raitakari, O.T., Rankinen, T., Rao, D.C., Rice, T.K., Ridker, P.M., Ritchie, M.D., Rudan, I., Salomaa, V., Samani, N.J., Saramies, J., Sarzynski, M.A., Schwarz, P.E., Shuldiner, A. R., Staessen, J.A., Steinthorsdottir, V., Stolk, R.P., Strauch, K., Tönjes, A., Tremblay, A., Tremoli, E., Vohl, M.-C., Völker, U., Vollenweider, P., Wilson, J.F., Witteman, J.C., Adair, L.S., Bochud, M., Boehm, B.O., Bornstein, S.R., Bouchard, C., Cauchi, S., Caulfield, M.J., Chambers, J.C., Chasman, D.I., Cooper, R.S., Dedoussis, G., Ferrucci, L., Froguel, P., Grabe, H.-J., Hamsten, A., Hui, J., Hveem, K., Jöckel, K.-H., Kivimaki, M., Kuh, D., Laakso, M., Liu, Y., März, W., Munroe, P.B., Njølstad, I., Oostra, B.A., Palmer, C.N., Pedersen, N.L., Perola, M., Pérusse, L., Peters, U., Power, C., Quertermous, T., Rauramaa, R., Rivadeneira, F., Saaristo, T.E., Saleheen, D., Sinisalo, J., Slagboom, P.E., Snieder, H., Spector, T.D., Stefansson, K., Stumvoll, M., Tuomilehto, J., Uitterlinden, A.G., Uusitupa, M., van der Harst, P., Veronesi, G., Walker, M., Wareham, N.J., Watkins, H., Wichmann, H.-E., Abecasis, G. R., Assimes, T.L., Berndt, S.I., Boehnke, M., Borecki, I.B., Deloukas, P., Franke, L., Frayling, T.M., Groop, L.C., Hunter, D.J., Kaplan, R.C., O'Connell, J.R., Qi, L., Schlessinger, D., Strachan, D.P., Thorsteinsdottir, U., van Duijn, C.M., Willer, C.J., Visscher, P.M., Yang, J., Hirschhorn, J.N., Zillikens, M.C., McCarthy, M.I., Speliotes, E.K., North, K.E., Fox, C.S., Barroso, I., Franks, P.W., Ingelsson, E., Heid, I. M., Loos, R.J., Cupples, L.A., Morris, A.P., Lindgren, C.M., Mohlke, K.L., 2015. New genetic loci link adipose and insulin biology to body fat distribution. Nature 518, 187–196.
Song, Y., Milon, B., Ott, S., Zhao, X., Sadzewicz, L., Shetty, A., Boger, E.T., Tallon, L.J., Morell, R.J., Mahurkar, A., Hertzano, R., 2018. A comparative analysis of library prep approaches for sequencing low input translatome samples. BMC Genom. 19, 696.
Soták, M., Rajan, M.R., Clark, M., Biörserud, C., Wallenius, V., Hagberg, C.E., Börgeson, E., 2022. Healthy subcutaneous and omental adipose tissue is associated with high expression of extracellular matrix components. Int. J. Mol. Sci. 23.
Stefan, N., 2020. Causes, consequences, and treatment of metabolically unhealthy fat distribution. Lancet Diabetes Endocrinol. 8, 616–627.
Tchernof, A., Després, J.-P., 2013. Pathophysiology of human visceral obesity: an update. Physiol. Rev. 93, 359–404.
The genotype-tissue expression (GTEx) project. Nat. Genet. 45, 2013, 580–585.
Voisin, S., Almén, M.S., Zheleznyakova, G.Y., Lundberg, L., Zarei, S., Castillo, S., Eriksson, F.E., Nilsson, E.K., Blüher, M., Böttcher, Y., Kovacs, P., Klovins, J., Rask-Andersen, M., Schiöth, H.B., 2015. Many obesity-associated SNPs strongly associate with DNA methylation changes at proximal promoters and enhancers. Genome Med. 7, 103.
Wajchenberg, B.L., 2000. Subcutaneous and visceral adipose tissue: their relation to the metabolic syndrome. Endocr. Rev. 21, 697–738.
Zhong, J., Zareifi, D., Weinbrenner, S., Hansen, M., Klingelhuber, F., Nono Nankam, P.A., Frendo-Cumbo, S., Bhalla, N., Cordeddu, L., Castro Barbosa, T. de, Arner, P., Dahlman, I., Muniandy, M., Heinonen, S., Pietiläinen, K.H., Hoffmann, A., Ghosh, A., John, D., Tönjes, A., Ståhl, P.L., Böttcher, Y., Keller, M., Kovacs, P., Kerr, A.G., Langin, D., Wolfrum, C., Blüher, M., Krahmer, N., Massier, L., Mejhert, N., Rydén, M., 2025. adiposetissue.org: a knowledge portal integrating clinical and experimental data from human adipose tissue. Cell Metab. 37, 566–569.